

PACS numbers: 42.65.–k; 42.70.Nq; 42.40.Eq
DOI: 10.1070/QE2005v035n02ABEH002864

Vector two-wavelength interaction on reflection holographic gratings in cubic gyrotropic photorefractive crystals

A.M. Plesovskikh, S.M. Shandarov, A.G. Mart'yanov, A.E. Mandel',
N.I. Burimov, E.A. Shaganova, Yu.F. Kargin, V.V. Volkov, A.V. Egorysheva

***Abstract*. The interaction of two counterpropagating light waves on reflection holographic gratings is studied in cubic photorefractive crystals with the natural optical activity. The anisotropy of contributions from intramode (without a change in the refractive index of natural circularly polarised waves) and intermode processes to the interaction of the waves in a bismuth titanate crystal is considered. It is shown that the polarisation dependences of the effective gain and the polarisation vectors of the interacting light beams measured at a wavelength of 633 nm in a (100) cut $Bi_{12}TiO_{20}$: Fe, Cu crystal of thickness 2.6 mm well agree with numerical calculations with the use of the two-beam coupling constant equal to 6.8 cm^{-1}.**

Keywords: *photorefractive grating, two-wave interaction, bismuth titanate.*

1. Introduction

Photorefractive cubic sillenite $Bi_{12}MO_{20}$ crystals (M = Ge, Si, Ti) are characterised by fast nonlinear response and possess the natural optical activity [1, 2]. Interest in these crystals is related to their applications in dynamic holography devices [1]. Holographic gratings are often recorded and the interaction of light beams on them is investigated by using the interaction of two copropagating beams intersecting in a crystal at an angle that is substantially smaller than 90°. However, the maximum interaction efficiency (in the absence of an external electric field) can be obtained in the case of counterpropagating beams. In this case, the amplitude of a photorefractive grating produced due to the diffusion mechanism in the absence of saturation of traps is inversely proportional to its period [1]. An advantage of reflection gratings, the efficient two-wave interaction on which in sillenite crystals was demonstrated in papers [3 – 9], is the possibility of their simple production when the signal beam is produced from the pump beam reflected from the output face [3]. This substantially reduces the dependence of the interaction of light waves on external factors such as vibrations of the elements of an optical scheme. Reflection gratings and schemes based on them can be used for the development of narrowband optical filters [10], holographic interferometers [4], and other practical applications.

The vector interaction of light waves on phase reflection gratings in photorefractive sillenite crystals was considered in paper [11] in the undepleted pump approximation. The scalar model of interaction of counterpropagating linearly polarised waves taking a change in the pump power into account but neglecting the transformation of their polarisation state was used [3] to analyse the formation dynamics of a reflection grating in a (100) cut $Bi_{12}TiO_{20}$ crystal. The two-beam interaction of circularly polarised waves in the (111) cut of a cubic gyrotropic photorefractive crystal on a reflection grating having the phase and amplitude components was studied in paper [6].

In this paper, we analyse the two-wave interaction on reflection holographic gratings in cubic crystals under the conditions of transformation of the polarisation state of the light field due to the natural optical activity and self-action effects. The general relations obtained below take into account the anisotropy of electrooptical and photoelastic contributions to the phase modulation of the optical properties of the medium by the spatial-charge field of the grating and its absorption component, as well as the effects of light absorption and pump depletion.

2. General equations

Consider the interaction of signal (s) and pump (p) light waves with the normal vectors $\boldsymbol{n}_s$ and $\boldsymbol{n}_p$ propagating in the opposite directions parallel to the x axis in a cubic photorefractive crystal (Fig. 1) of the symmetry class 23. In the absence of external fields in the case of weak optical absorption, the light fields of these waves can be written, due to the natural optical activity of the crystal, as a superposition of circularly polarised waves [11]:

$$\boldsymbol{E}_p(x) = \{C_{p1}(x)\boldsymbol{e}_1 \exp(-ik_0 n_1 x) + C_{p2}(x)\boldsymbol{e}_2 \exp(-ik_0 n_2 x)\} \exp\left(-\tfrac{1}{2}\alpha x\right), \quad (1)$$

A.M. Plesovskikh, S.M. Shandarov, A.G. Mart'yanov, A.E. Mandel', N.I. Burimov, E.A. Shaganova Tomsk State University of Control Systems and Radioelectronics, prosp. Lenina 40, 634050 Tomsk, Russia; e-mail: shand@stack.ru, martalex@ed.rk.tusur.ru, mae@svch.rk.tusur.ru, bnik@online.tomsk.net, kora@mail.ru;
Yu.F. Kargin, V.V. Volkov, A.V. Egorysheva N.S. Kurnakov Institute of General and Inorganic Chemistry, Russian Academy of Sciences, Leninsky prosp. 31, 117907 Moscow, Russia; e-mail: yu.kargin@rambler.ru, v.volkov@rambler.ru

Received 15 September 2004
Kvantovaya Elektronika **35** (2) 163 – 168 (2005)
Translated by M.N. Sapozhnikov

$$\boldsymbol{E}_s(x) = \{C_{s1}(x)\boldsymbol{e}_1^* \exp(ik_0 n_1 x) + C_{s2}\boldsymbol{e}_2^* \exp(ik_0 n_2 x)\} \exp\left(\tfrac{1}{2}\alpha x\right), \quad (2)$$

where $\boldsymbol{e}_{1,2} = (\boldsymbol{y}_0 \pm i\boldsymbol{z}_0)/\sqrt{2}$ are the unit vectors corresponding to the left and right circular polarisations; $n_{1,2} = n_0 \pm \rho/k_0$ are the refractive indices of natural waves; $k_0 = 2\pi/\lambda$ is the wave number in vacuum; n_0 and α are the refractive index and absorption coefficient of the unperturbed crystal; and ρ is its specific rotary power.

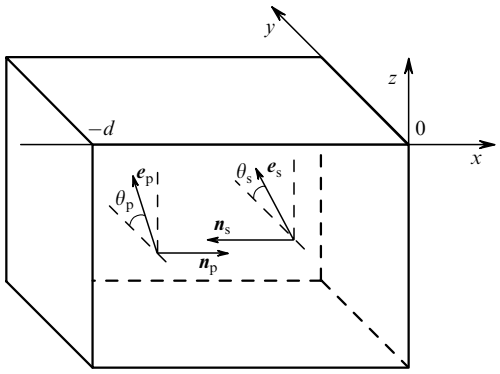

Figure 1. Geometry of the interaction of the counterpropagating signal (s) and pump (p) light waves in a cubic gyrotropic photorefractive crystal.

The interference pattern produced by the signal and pump waves in the crystal has the lattice vector $\boldsymbol{K} = 2k_0 n_0 \boldsymbol{x}_0$ and the intensity distribution

$$I(x) = I_0(x)\left[1 + \frac{m(x)}{2}\exp(iKx) + \frac{m^*(x)}{2}\exp(-iKx)\right], \quad (3)$$

where $K = |\boldsymbol{K}| = 2\pi/\Lambda$; Λ is the spatial period of the interference pattern; and its average intensity I_0 and contrast m are determined by the expressions

$$I_0(x) = \left[|C_{p1}(x)|^2 + |C_{p2}(x)|^2\right]\exp(-\alpha x) + \left[|C_{s1}(x)|^2 + |C_{s2}(x)|^2\right]\exp(\alpha x), \quad (4)$$

$$m(x) = 2\,\frac{C_{s1}(x)C_{p2}^*(x) + C_{s2}(x)C_{p1}^*(x)}{I_0(x)}. \quad (5)$$

The nonuniform illumination of the crystal leads to the nonuniform excitation of charge carriers. By moving in the crystal due to the diffusion redistribution mechanism, they form the grating of the spatial-discharge field. For the case $m \ll 1$, we can assume that this field contains only the first spatial harmonic with the period $\Lambda = \lambda/2n_0$, which is shifted by one fourth of this period with respect to the interference pattern [1], and the amplitude of the harmonic linearly depends on the contrast:

$$E_1(x,t) = -im(x)E_{sc}(t), \quad (6)$$

where the field formation dynamics is determined by the function $E_{sc}(t)$ depending on the distribution mechanism of charge carriers. Because crystals of the symmetry 23 possess piezoelectric properties, their photorefractive response will depend on the electrooptical and photoelastic effects [12]. Due to a complex structure of defect centres, the amplitude gratings caused by photoinduced changes in light absorption can be also formed in the crystal [13–15].

In the linear approximation in the contrast m, the amplitude of the first spatial harmonic of the absorption grating can be represented in the form $\Delta\alpha_1(x,t) = m(x)\,\alpha_g(t)$, where $\alpha_g(t)$ is a parameter characterising spatially inhomogeneous photoinduced changes in absorption in the crystal. Taking into account the local relation between the absorption component of the grating and the interference pattern and also the contributions from electrooptical and photoelastic effects to its phase component, we represent the relative dielectric constant of the crystal at the light wave frequency in the form

$$\varepsilon(x,t) = \varepsilon^0 + \frac{\Delta\varepsilon^{ph}(x,t)}{2}\exp(iKx) + \frac{\Delta\varepsilon^{ph^*}(x,t)}{2}\exp(-iKx) + \frac{\Delta\varepsilon^{a}(x,t,m)}{2}\exp(iKx) + \frac{\Delta\varepsilon^{a}(x,t,m^*)}{2}\exp(-iKx). \quad (7)$$

Taking into account the relations presented in [12, 16], the components of the tensors ε^0, $\Delta\varepsilon^{ph}$, and $\Delta\varepsilon^a$ for the unperturbed crystal and perturbations of the dielectric constant induced in the crystal are determined by the expressions

$$\varepsilon_{mn}^0 = \left(n_0^2 - i\,\frac{n_0\alpha}{k_0}\right)\delta_{mn} - i\,\frac{2n_0\rho}{k_0}\,\delta_{mnp}m_p, \quad (8)$$

$$\Delta\varepsilon_{mn}^{ph} = im\left(n_0^4 r_{41}^S E_{sc}\Delta b_{mn}\right), \Delta\varepsilon_{mn}^{a}(m) = -im\left(\frac{n_0}{k_0}\,\alpha_g\delta_{mn}\right), \quad (9)$$

$$\Delta b_{mn} = \left[|\delta_{mnp}|p_p + \frac{1}{r_{41}^S}\left(P_{mnkl}^E p_l\gamma_{ki}e_{pir}p_p p_r\right)\right], \quad (10)$$

where δ_{mn} is the unit symmetric tensor of the second order; δ_{mnp} is the unit antisymmetric tensor of the third order; $p_{p,r,l}$ are the direction cosines of the lattice vector $\boldsymbol{K}||\boldsymbol{x}_0$; r_{41}^S and P_{mnkl}^E are the components of the electrooptical tensor of a clamped crystal and the photoelastic tensor measured in a constant electric field; γ_{ki} are the components of the tensor inverse to $\Gamma_{ik} = C_{ijkl}^E p_j p_l$; and C_{ijkl}^E and e_{pir} are the components of the tensors of elasticity moduli and piezoelectric constants.

By using the method of slowly varying amplitudes and the relations presented above, we can obtain from the wave equation for cubic gyrotropic crystals the equations for coupled waves, which describe the interaction of the signal and pump waves on the reflection holographic grating,

$$\frac{dC_{s1}}{dx} = -\frac{\gamma}{4}\,m\left[g_I^* C_{p1}\exp(-i2\rho x) + (g_E - g_a)C_{p2}\right]\exp(-\alpha x), \quad (11)$$

$$\frac{dC_{s2}}{dx} = -\frac{\gamma}{4}\,m\left[(g_E - g_a)C_{p1} + g_I C_{p2}\exp(i2\rho x)\right]\exp(-\alpha x), \quad (12)$$

$$\frac{dC_{p1}}{dx} = -\frac{\gamma}{4} m^* \left[g_I C_{s1} \exp(i2\rho x) + (g_E + g_a) C_{s2} \right] \exp(\alpha x), \quad (13)$$

$$\frac{dC_{p2}}{dx} = -\frac{\gamma}{4} m^* \left[(g_E + g_a) C_{s1} + g_I^* C_{s2} \exp(-i2\rho x) \right] \exp(\alpha x), \quad (14)$$

where $\gamma = k_0 n_0^3 r_{41}^S E_{sc}$ are the coupling constants; $g_I = \boldsymbol{e}_1^* \Delta \boldsymbol{b} \boldsymbol{e}_2$ and $g_E = \boldsymbol{e}_1^* \Delta \boldsymbol{b} \boldsymbol{e}_1 = \boldsymbol{e}_2^* \Delta \boldsymbol{b} \boldsymbol{e}_2$ are the tensor convolutions describing the contributions of intramode (without variations in the intrinsic refractive index) and intermode processes, respectively, to the interaction of counterpropagating waves; and $g_a = \alpha_g / (k_0 n_0^3 r_{41}^S E_{sc})$ is the coefficient describing the relative contribution of the absorption grating to the two-beam interaction.

The system of equations (11)–(14) can be used to analyse the two-wave interaction on reflection holographic gratings in cubic photorefractive crystals for arbitrary polarisation of light beams.

3. Anisotropy of contributions from intramode and intermode processes to the interaction

The coefficients g_I, g_E, and g_a entering Eqns (11)–(14) determine the efficiency and polarisation characteristics of the interaction of signal and pump waves on the reflection grating. The absorption grating makes a contribution to the intermode process of two-beam coupling accompanied by a change in the intrinsic refractive index. The coefficient g_a characterising this contribution is a real quantity, which is independent of the orientation of the lattice vector $\boldsymbol{K}$ with respect to the crystallographic coordinate system. The anisotropy of the electrooptical effect and secondary photoelastic effect leads to the orientation dependence of another real coefficient g_E contributing to intermode processes. To analyse this dependence, we will define the orientation of the x axis, coinciding with the vector $\boldsymbol{K}$ of the xyz coordinate system (Fig. 1), with respect to the [001] and [100] crystallographic axes with the help of spherical coordinate angles β and α. We assume that the z axis always lies in the (001) plane, while the y axis is oriented in the plane in which the lattice vector $\boldsymbol{K}$ and the [001] axis are located (Fig. 2).

The dependences of g_E on the orientation angle β calculated for the bismuth titanate crystal for some constant angles α taking the crystal symmetry into account completely characterise the anisotropy of this crystal (Fig. 3a). It follows from Fig. 3a that, when the reflection grating vector is oriented in crystallographic planes of the type {100} [i.e., (100), (010), and (001)], the contribution of the phase (photorefractive) component of the grating to the intermode processes is absent. This contribution achieves the maximum values when the vector $\boldsymbol{K}$ is oriented in planes of the type {110} along the crystallographic directions of the type ⟨111⟩.

The anisotropy of the coefficient $g_I = |g_I| \exp(i\varphi_I)$ contribution to intramode processes, which is a complex quantity in the general case, is illustrated in Figs 3b, c, where the orientation dependences of its modulus and argument are presented for the bismuth titanate crystal. The modulus of the coefficient g_I achieves the maximum

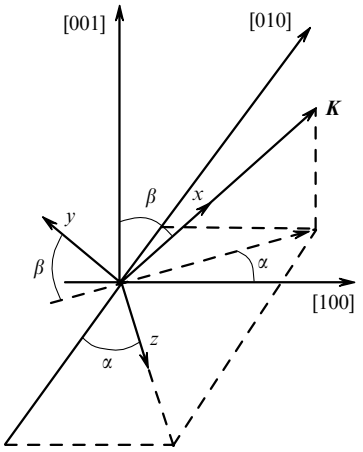

Figure 2. Orientation of the axes of the working xyz coordinate system (Fig. 1) with respect to the crystallographic axes.

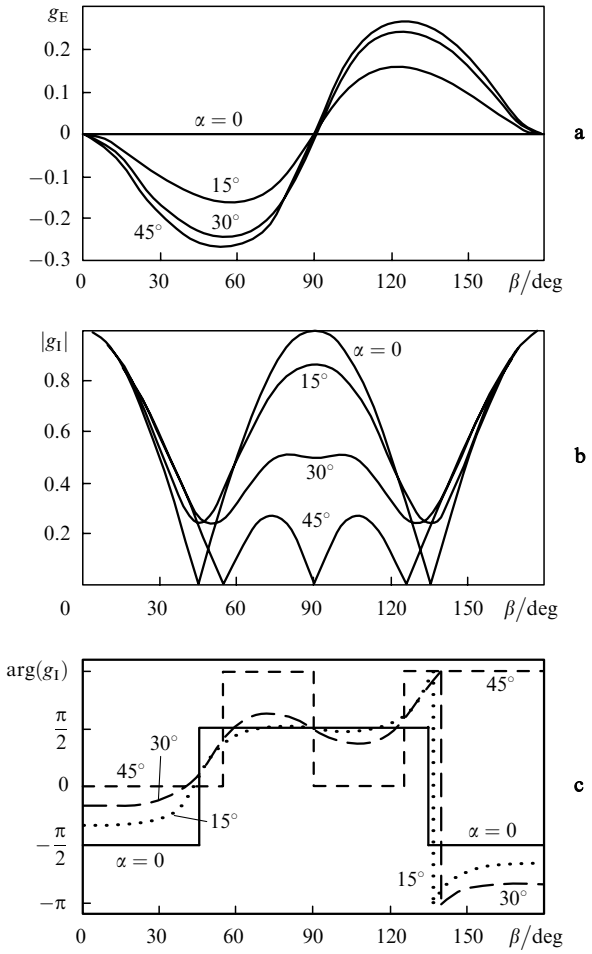

Figure 3. Dependences of the real coefficient g_E characterising the efficiency of intermode processes (a) and the modulus (b) and argument (c) of the coefficient g_I, characterising intramode processes, on the angle β between the lattice vector and the [001] crystallographic axis for different orientation angles α.

when the lattice vector is oriented along the crystallographic directions of the type ⟨100⟩ (Fig. 3b). In this case, the coupling of counterpropagating waves interacting on the reflection grating, caused by its photorefractive component, occurs only due to intramode processes ($|g_I| = 1$, $g_E = 0$).

When the vector $\boldsymbol{K}$ is oriented along the $\langle 111 \rangle$ direction, this component makes no contribution to intramode processes, whereas the intermode coupling coefficient takes the extreme values ($g_E = \pm 0.266$, see Fig. 3a). Note that the phase component of the reflection grating does not lead to the interaction of the waves when the vector $\boldsymbol{K}$ oriented along the crystallographic $\langle 110 \rangle$ directions ($|g_I| = 0$, $g_E = 0$). For such a cut of a cubic photorefractive crystal, the counterpropagating waves can interact only on the amplitude (absorption) component of the reflection grating.

The modulus of the coefficient g_I is determined only by the orientation of the x axis, coinciding with the direction of the lattice vector, and is independent of the orientation of the y and z axes with respect to the crystallographic coordinate system (Fig. 2). However, the argument φ_I of the coefficient g_I is not invariant with respect to the choice of axes y and z because the phases of complex amplitudes of the natural waves entering the equations, which characterise their polarisation state, also depend on the orientation of these axes. The orientation dependences presented in Fig. 3c demonstrate the behaviour of the coefficient g_I for the selected coordinate system xyz (see Fig. 2). In this case, the coefficient g_I is purely imaginary when the reflection grating vector is oriented in crystallographic planes of the type $\{100\}$, and it is purely real for planes of the type $\{110\}$. The anisotropy of the coefficients g_E and g_I was analysed by using the material parameters of the bismuth titanate crystal from [17].

4. Two-beam interaction of linearly polarised waves

It follows from Eqns (11)–(14) and (6) that the amplitudes of linearly polarised interacting waves satisfy the conditions $C_{p1}(x) = C^*_{p2}(x) = C_p(x)$ and $C_{s1}(x) = C^*_{s2}(x) = C_s(x)$ and can be represented in the form

$$C_{p1,2}(x) = |C_p(x)| \exp[\mp i\varphi_p(x)],$$
$$C_{s1,2}(x) = |C_s(x)| \exp[\pm i\varphi_s(x)]. \tag{15}$$

In this case, the contrast of the interference pattern in the crystal, determined by (6), is a real function of the coordinate x:

$$m(x) = 2\,\frac{C_s(x)C_p(x) + C^*_s(x)C^*_p(x)}{I_0(x)} = 2\,\frac{|C_s(x)||C_p(x)|\cos[\varphi_s(x) - \varphi_p(x)]}{|C_p(x)|^2 \exp(-\alpha x) + |C_s(x)|^2 \exp(\alpha x)}, \tag{16}$$

and Eqns (11)–(14) for the coupled waves are reduced to the two equations

$$\frac{dC_s}{dx} = -\frac{\gamma}{4}\, m\{|g_I|C_p \exp[-i(2\rho x + \varphi_I)] + (g_E - g_a)C^*_p\} \exp(-\alpha x), \tag{17}$$

$$\frac{dC_p}{dx} = -\frac{\gamma}{4}\, m\{|g_I|C_s \exp[i(2\rho x + \varphi_I)] + (g_E + g_a)C^*_s\} \exp(\alpha x). \tag{18}$$

By passing to the intensities $\tilde{I}_s(x) \sim [|C_{s1}(x)|^2 + |C_{s2}(x)|^2] \times \exp(\alpha x)$ and $\tilde{I}_p(x) \sim [|C_{p1}(x)|^2 + |C_{p2}(x)|^2] \exp(-\alpha x)$ of signal and pump waves in the crystal, respectively, we obtain from the system of equations (17) and (18)

$$\frac{\partial \tilde{I}_s}{\partial x} = \alpha \tilde{I}_s - \gamma[|g_I| \cos(2\rho x + \varphi_I + \varphi_s + \varphi_p) + (g_E - g_a)\cos(\Delta\varphi)]\cos(\Delta\varphi)\frac{\tilde{I}_s \tilde{I}_p}{\tilde{I}_s + \tilde{I}_p}, \tag{19}$$

$$\frac{\partial \tilde{I}_p}{\partial x} = -\alpha \tilde{I}_p - \gamma[|g_I| \cos(2\rho x + \varphi_I + \varphi_s + \varphi_p) + (g_E + g_a)\cos(\Delta\varphi)]\cos(\Delta\varphi)\frac{\tilde{I}_s \tilde{I}_p}{\tilde{I}_s + \tilde{I}_p}, \tag{20}$$

$$\frac{\partial \varphi_s}{\partial x} = \frac{\gamma}{2}[|g_I| \sin(2\rho x + \varphi_I + \varphi_s + \varphi_p) + (g_E - g_a)\sin(\Delta\varphi)]\cos(\Delta\varphi)\frac{\tilde{I}_p}{\tilde{I}_s + \tilde{I}_p}, \tag{21}$$

$$\frac{\partial \varphi_p}{\partial x} = \frac{\gamma}{2}[|g_I| \sin(2\rho x + \varphi_I + \varphi_s + \varphi_p) - (g_E + g_a)\sin(\Delta\varphi)]\cos(\Delta\varphi)\frac{\tilde{I}_s}{\tilde{I}_s + \tilde{I}_p}, \tag{22}$$

where $\Delta\varphi = \varphi_s - \varphi_p$.

Equations (19)–(22) completely describe the interaction of linearly polarised counterpropagating waves for an arbitrarily oriented crystal taking into account the electrooptical and photoelastic effects and diffraction from the absorption grating.

When the contribution of the absorption grating to the interaction is negligibly small, we obtain from Eqns (19) and (20)

$$\frac{1}{\tilde{I}_s \tilde{I}_p}\frac{d(\tilde{I}_s \tilde{I}_p)}{dx} = -\gamma[|g_I| \cos(2\rho x + \varphi_I + \varphi_s + \varphi_p) + g_E \cos(\Delta\varphi)]\cos(\Delta\varphi). \tag{23}$$

The integration of this expression gives the result

$$\tilde{I}_s(x)\tilde{I}_p(x) = \tilde{I}_s(0)\tilde{I}_p(0) \exp\left\{-\gamma \int_0^x [|g_I| \cos(2\rho x + \varphi_I + \varphi_s + \varphi_p) + g_E \cos(\Delta\varphi)]\cos(\Delta\varphi)dx\right\}, \tag{24}$$

which allows us to introduce the effective gain for the interaction of the counterpropagating waves in a crystal of thickness d in the form

$$\Gamma_{eff} = \frac{\gamma}{d}\int_{-d}^{0} [|g_I| \cos(2\rho x + \varphi_I + \varphi_s + \varphi_p) + g_E \cos(\Delta\varphi)]\cos(\Delta\varphi)dx. \tag{25}$$

Note that this coefficient can be expressed in terms of the intensities of the interacting waves

$$\Gamma_{\text{eff}} = \frac{1}{d} \ln \left\{ \frac{\tilde{I}_s(-d)\tilde{I}_p(-d)}{\tilde{I}_s(0)\tilde{I}_p(0)} \right\}, \quad (26)$$

which in turn can be readily determined experimentally. The coefficient Γ_{eff} characterises the efficiency of the vector interaction of counterpropagating waves on the phase reflection grating and is independent of the absorption of light in the crystal and variations in absorption during the grating formation [3].

5. Polarisation dependences for the interaction of linearly polarised waves on phase gratings in the (100) cut

The results of numerical integration of the system of equations (19)–(22) for phase gratings produced in the (100) cut bismuth titanate crystals ($g_I = i$, $g_E = 0$) are shown in Fig. 4. We used in the calculations the value of the specific rotary power $\rho = -6.34$ deg mm^{-1}, which is typical for bismuth titanate at a wavelength of 633 nm. The absorption coefficient and the coupling constant were $\alpha = 2.3$ cm^{-1} and $\gamma = 6.8$ cm^{-1}, respectively. We assumed that the phase holographic grating was produced upon the interaction of the incident pump beam with the signal beam reflected from the output face of the crystal ($x = 0$), and the input face ($x = -d$) had an AR coating (Fig. 1). In this case, the intensities and phases of the interacting waves for $x = 0$ are related by the expressions $\tilde{I}_s(0) = \tilde{I}_p(0)R^2$ and $\varphi_s(0) = \varphi_p(0) = \theta_{P0}$, which were used as initial conditions in the integration of Eqns (19)–(22). Here, R is the Fresnel reflection coefficient for the normal incidence of light and θ_{P0} is the angle between the polarisation vector of the light field on the output face of the crystal and the y axis of the coordinate system (Fig. 1).

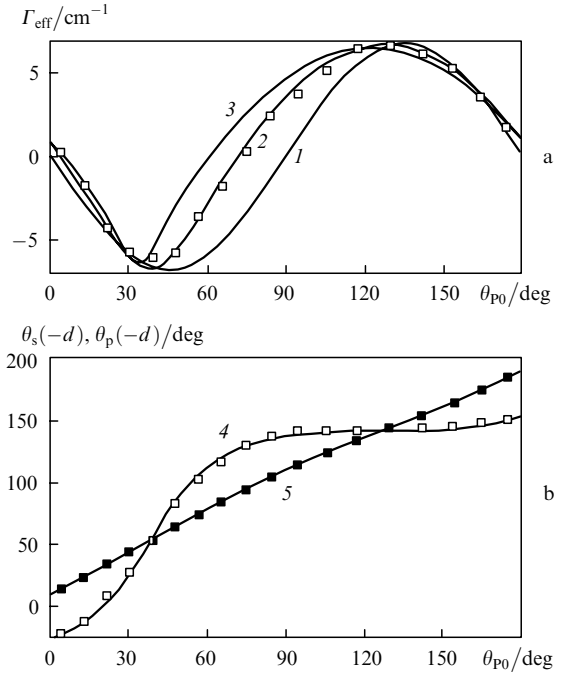

Figure 4. Dependences of the effective gain for the interaction of counterpropagating waves (a) and the polarisation angles (b) of the signal (*4*) and pump (*5*) waves on the input face ($x = -d$) on the angle θ_{P0} characterising the orientation of the polarisation vector of the light field on the output face ($x = 0$) for the $Bi_{12}TiO_{20}$: Fe, Cu crystal of thickness $d = 0.1$ (*1*), 2.6 (*2*, *4*, *5*), and 5.0 mm (*3*). The solid curves correspond to the theory, squares – to the experiment.

The dependences of the effective gain on the 'output' angle θ_{P0} calculated by the results of numerical analysis according to expression (26) for crystals of widths $d = 0.1$, 2.6, and 5.0 mm are presented in Fig. 4a. One can see that the gain maximum ($\Gamma_{\text{eff}} = 6.8$ cm^{-1}) is achieved in the crystal of thickness $d = 0.1$ mm for $\theta_{P0} = 135^\circ$. For the polarisation angle $\theta_{P0} = 45^\circ$, the gain achieves the same maximum but negative value, which corresponds to the maximum power transfer from the signal to pump beam. As d is increased, the extremum amplitudes decrease and for the negative values of ρ they shift to the lower angles θ_{P0}.

During the interaction of waves on the reflection grating, the orientation of the polarisation vectors of the waves also changes. The dependences of the polarisation angles $\theta_p(-d)$ and $\theta_s(-d)$, which characterise the pump and signal waves on the input face ($x = -d$), on the 'output' angle θ_{P0} for a crystal of thickness $d = 2.6$ mm are shown in Fig. 4b by solid curves. A comparison of the polarisation dependences in Figs 4a, b shows that the polarisation of the pump and signal waves on the input face is the same at the extreme values of the gain Γ_{eff}. The maximum additional optical rotation of the signal wave due to the interaction on the phase reflection grating takes place, on the contrary, when the effective gain is zero.

6. Experiment

We studied the polarisation dependences of the two-beam interaction of light at 633 nm on reflection gratings in a (100) cut $Bi_{12}TiO_{20}$: Fe, Cu single crystal of thickness $d =$ 2.6 mm. The crystal was grown from a melt, and according to the chemical analysis, the mass concentrations of iron and copper were 0.043 % and 0.0046 %, respectively. In the experiment, whose technique is described in papers [3, 6, 7], the interaction occurred on the reflection grating produced due the interference of the pump beam with the signal beam reflected from the output face ($x = 0$) of the crystal (Fig. 1). The slightly wedge-shaped ($\sim 1^\circ$) crystal provided the separation of the beams reflected from the input and output faces of the crystal. The polarisation and intensities of the pump beam propagated through the crystal and of the 'signal' beam reflected from the output face were measured after the establishment of a stationary regime.

The effective two-beam gain Γ_{eff} on the reflection grating was calculated from the experimental data by using expression (26) and the Fresnel reflection coefficient for the normal incidence of light. The calculated dependence of Γ_{eff} on the angle θ_{P0} determining the orientation of the polarisation vector of the light field on the 'output' face of the crystal is shown by squares in Fig. 4a. Good agreement between the experimental data and theoretical dependence suggests that the photorefractive grating produced upon the interaction of counterpropagating waves in the (100) cut $Bi_{12}TiO_{20}$: Fe, Cu crystal has the phase nature. The experimental dependences of the polarisation angles $\theta_p(-d)$ and $\theta_s(-d)$ on the 'output' angle θ_{P0} also agree with numerical calculations within the accuracy of measurements (Fig. 4b).

7. Conclusions

We have obtained the equations for coupled waves, which describe the vector two-beam interaction of the counter-

propagating waves on reflection gratings, which are produced in cubic photorefractive crystals possessing the natural optical activity. The anisotropy of contributions from the intramode (without a change in the refractive index of the natural circularly polarised waves) and intermode processes to the interaction of the waves in the bismuth titanate crystal has been analysed. The equations have been obtained for linearly polarised waves, which completely describe the interaction of counterpropagating waves in an arbitrarily oriented crystal taking into account the electrooptical and photoelastic effects and diffraction from the absorption grating. The numerical integration of these equations for the (100) cut bismuth titanate crystal in the case of a negligible small absorption grating has shown that the maximum value of the effective gain decreases with increasing crystal thickness. The experimental polarisation dependences of the gain and polarisation vectors of the light beams interacting in the $Bi_{12}TiO_{20}$: Fe, Cu crystal well agree with the theoretical results.

Acknowledgements. This work was supported by the Russian Foundation for Basic Research (Grant No. 02-02-81044) and INTAS (Grant No. 1B 481).

References

1. Petrov M.P., Stepanov S.I., Khomenko A.V. *Fotorefractivnye kristally v kogerentnoi optike* (Photorefractive Crystals in Coherence Optics) (St. Petersburg: Nauka, 1992).
2. Odulov S.G., Soskin M.S., Khizhnyak A.I. *Lazery na dinamicheskikh reshetkakh* (Lasers on Dynamic Gratings) (Moscow: Nauka, 1990).
3. Ageev E.Yu., Shandarov S.M., Vereteennikov S.Yu., Mart'yanov A.G., Kartashov V.A., Kamshilin A.A., Prokof'ev V.V., Shepelevich V.V. *Kvantovaya Elektron.*, **31**, 343 (2001) [*Quantum Electron.*, **31**, 343 (2001)].
4. Kukhtatev N.V., Chen B.S., Venkateswarlu P., Salamo G., Klein M. *Opt. Commun.*, **104**, 23 (1993).
5. Mallick S., Miteva M., Nikolova L. *J. Opt. Soc. Am. B*, **14**, 1179 (1997).
6. Mart'yanov A.G., Ageev E.Yu., Shandarov S.M., Mandel' A.E., Bochanova N.V., Ivanova N.V., Kargin Yu.F., Volkov V.V., Egorysheva A.V., Shepelevich V.V. *Kvantovaya Elektron.*, **33**, 226 (2003) [*Quantum Electron.*, 33, 226 (2003)].
7. Martyanov A.G., Antonova N.Yu., Shandarov S.M., Kargin Yu.F., Volkov V.V., Egorysheva A.V., Prokofiev V.V. *ICO Topical Meeting on Polarization Optics* (Joensuu, Finland, 2003) p. 220.
8. Von Bally G., Thien R., Kemper B. *Ukr. J. Phys.*, **49**, 457 (2004).
9. Lichtenberg S., Petrov V.M., Petter G., Tschudi T., Chamrai A.V., Petrov M.P. *Ukr. J. Phys.*, **49**, 467 (2004).
10. Kanaev I.F., Malinovskii V.K., Surovtsev N.V. *Fiz. Tverd. Tela*, **42**, 2079 (2000).
11. Mart'yanov A.G., Shandarov S.M., Litvinov R.V. *Fiz. Tverd. Tela*, **44**, 1006 (2002).
12. Volkov V.I., Kargin Yu.F., Kukhtarev N.V., Privalko A.V., Semetets T.I., Shandarov S.M., Shepelevich V.V. *Kvantovaya Elektron.*, **18**, 1237 (1991) [*Sov. J. Quantum Electron.*, **21**, 1122 (1991)].
13. Tayebati P., Mahgerefteh D. *J. Opt. Soc. Am. B*, **8**, 1053 (1991).
14. Kamshilin A.A. *Opt. Commun.*, **93**, 350 (1992).
15. Shandarov S., Emelyanov A., Kobozev O., Reshet'ko A., Volkov V., Kargin Yu. *Proc. SPIE Int. Soc. Opt. Eng.*, **2801**, 221 (1996).
16. Sturman B.I., Podivilov E.V., Kamenev V.P., Nippolainen E., Kamshilin A.A. *Zh. Eksp. Teor. Fiz.*, **119**, 125 (2001).
17. Kobozev O.V., Shandarov S.M., Litvinov R.V., Maksimov A.A., Kargin Yu.F., Volkov V.V. *Neorg. Mater.*, **34**, 1486 (1998).